Available online at www.sciencedirect.com

ScienceDirect

Procedia Engineering 10 (2011) 2123–2128

Engineering Procedia

ICM11

Investigation of damage evolution in short glass fibers reinforced polyamide 6,6 under tensile loading using infrared thermography

A. Ghorbel [1,2], N. Saintier [2,*], A. Dhiab [1]

[1] *Unit of mechanics, modelling and production U2MP-ENIS, BPW 3038 Sfax-Tunisia.*
[2] *Arts et Métiers ParisTech (centre de Bordeaux-Talence), I2M-DUMAS, UMR 5295, Esplanade des Arts et Métiers 33405 TALENCE CEDEX FRANCE*

Abstract

Mechanical properties of polymers are very sensitive to environmental conditions in particular temperature. In the case of mechanical testing, thermomechanical coupling induce heat sources to be activated during the deformation and damage processes so that the temperature of the specimen may vary during testing. Depending on the characteristic temporal and spacial scales of the deformation and damage processes involved by the loading this temperature increase might be uniform or highly localized. The aim of the study is to investigate the temperature field evolution of glass fibers reinforced polyamide 6,6 with 0% (PA66GF00), 10% (PA66GF10), 20% (PA66GF20) and 30% (PA66GF30) glass fiber. In addition to infrared thermography, digital image correlation (DIC) was used to quantify deformation localization zones and correlate them to identified heat dissipation sources. Until necking, the heat distribution was found to be nearly homogeneous on PA66GF00 with a well marked thermoelastic region, succeeded by an homogeneous heat increase due to viscoplastic dissipation. Necking is associated to strong heat increase that is localized on the the necking area. The thermal response of short fiber reinforced materials was found to differ markedly from the uncharged one. Strong heterogeneity of the thermal was observed and was associated to localisation processes at different scales (investigated by DIC). The effect of the applied strain rate on the observed thermal heterogenities was investigated. In addition to DIC, the volume damage evolution was monitored using X-ray computed microtomography in particular region.

Keywords : Polyamide 6,6 ; micro-shear, infrared thermography, microtomography, damage.

* Corresponding author. Tel.: +33 5 56 84 53 61 fax: +33 5 56 84 53 66.
E-mail address: nicolas.saintier@ensam.eu

 doi:10.1016/j.proeng.2011.04.351

1. Introduction

During the past several years, an increasing amount of attention has been given to the mechanical behaviour of engineering thermoplastics and their composites. One reason for this interest is that engineering thermoplastics are finding increasing number of applications in many structural automotive components. Polyamide-6,6 is one such engineering thermoplastic which is known for its balance of strength, modulus and chemical resistance. Both polyamide-6,6 and short E-glass fibre reinforced polyamide- 6,6 composite have many potential applications, such as stressed functional automotive parts (fuel injection rails, steering column switches), safety parts in sports and leisure (snowboard bindings) and other commercial products where creep resistance, stiffness, resistance to dynamic fatigue and some toughness are demanded in addition to weight saving. The E-glass fibres give the composite its stiffness and strength and polyamide-6,6 matrix provides the means for achieving toughness and chemical resistance in addition to holding the fibres together.

During the last few decades, the developments of infra-red cameras together with efficient image-processing methods have been successfully used for the thermo-mechanical analysis of the behaviour of numerous materials [1-4]. This non destructive analysis permits the surface temperature field to be measured and its evolution to be recorded. In relation to the mechanical (local or global) loading it offers a powerful tool for further understanding of thermomechanical coupling. Such couplings are also, X-ray tomography is a technique that has been originally developed for medical imaging, taking advantage of inhomogeneous absorption of X-rays in bodies. Now, due to the huge progresses that have been made in resolution (micron scale measurements are conceivable) and in 3D visualisation, X-ray computed microtomography (XCMT) becomes a power full tool for material sciences [5, 6] and 3D damage evaluation [7].

In this paper, using uniaxial tensile specimens, failure mechanisms of glass fibre reinforced and unreinforced polyamide-6,6 were studied using thermography infrared (IR) and X-ray computed microtomography. Scanning electron microscopy (SEM) analysis has been employed. The study also considered the effects of glass fibre weight fraction on the various failure mechanisms which lead to catastrophic fracture initiation.

2. Experimental procedures

2.1. Materials

The material used in this study is a commercial polyamide-6,6 and polyamide-6,6 containing 30 wt% glass-fibres (Heramid a nat and Heramid a nat FV030, provided by RADICI GROUP). They were used to produce moulded composites with 0, 10, 20 and 30% wt glass content (the glass fibre content was based on total mass of polymer). They were designed as PA66GF00, PA66GF10, PA66GF20 and PA66GF30. The specimens were made by injection moulding. Granulated commercial materials were held in a drying furnace at 80°C for 24h prior to injection. For all blends, the injection parameters were maintained constant. In order to test the material close to real service conditions, it was subjected to accelerated conditioning (moisture absorption) until equilibrium was reached with an ambient of 20°C and 50% relative humidity. Specimens have been conditioned after injection by drying them in a vacuum oven at 80°C for 24 h and then placed in a Voïtch Industrietechnik VC 4034 machine : temperature: 80°C and

relative humidity: 50). The weight of the specimens was monitored during this accelerated conditioning to ensure that equilibrium was reached. The water content at equilibrium was 2,2 % by weight.

2.2. *Mechanical testing*

The mechanical properties testing were performed using NF IN ISO 527-2 specimens (Fig. 1). The tensile tests were carried out at room temperature using a ZWICK/Roell Z250 tensile testing machine. A load cell with capacity of 10 KN was used to measure the applied load. The tests were carried out at different weight fractions: 0, 10, 20 and 30 wt% with constant relative humidity (50 RH). For each testing condition, several samples were used and at least three results were taken from those specimens in which the failure occurred within the gauge length. Yield strength, apparent modulus of elasticity, percent elongation and toughness values were determined by the tensile tests used most frequently when determining the mechanical properties of polymers.

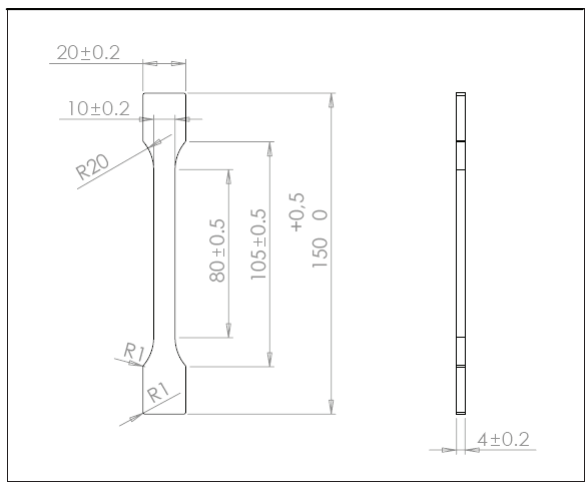

Fig. 1. specimen geometry

2.3. *Infrared thermography and digital image correlation*

Infrared thermography (IR) was used to determine real time evolution of the surface temperature field of materials in real time during tensile tests. The IR camera used in the study was a JADE 3 (FLIR system) set up at an acquisition frequency of 50 Hz. In addition to IR analyses, digital image correlation was used to identify strain localisation at the specimen surface. Two cameras where used, one high resolution camera (pixelfly) and on high speed camera in order to investigate the high speed localization process at the time of failure. CORELLI software developed at the ENS-Cachan was used to investigate the strain localisation processes.

2.4. *Tomography*

X-ray computed microtomography was used in order to investigate the damage state of the specimen after failure. In the present work, specimens after tensile test were examined in a Nanotom Phoenix

X-Ray machine at energy of 55 KeV using a 2304 × 2304 pixels camera. Several resolutions were used (7, 1.24 and 1.2 μm). Investigated areas were chosen from highly localizing zones identified from DIC or dissipating area identified from IR thermography.

3. Results

In the case of uncharged polymer, the stress-strain behaviour classically exhibit a quasi elastic behaviour followed by yielding and necking. Necking is associated to the development of two distinct strain localisation fronts that progress in opposite directions as shown figure 2.

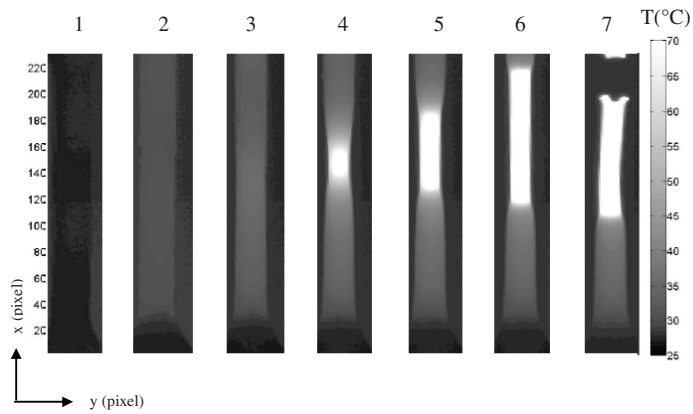

Fig. 2. Infrared thermography images sequence of PA66GF00 during tensile loading

In the case of reinforced polymers thermal response is different. Figure 3 illustrates a typical stress-time (dashed line) and corresponding mean thermal evolution at the specimen surface (solid line). The colour code of the background of the graph corresponds to the temperature along the central line of the specimen plotted as a function of time. The elastic phase is associated to a marked thermoelastic effect and temperature decrease. The end of the elastic phase is clearly observed on the mean thermal response. The instant corresponding to the maximum stress on the stress-time curve does not correspond to a macroscopic necking as it is the case for the pure PA66 material but to the development of microshear bands all along the specimen surface and that are clearly observable on the thermal images. Microshears develop at a direction close to 45° and have also been observed on the DIC images (Figure 4). The microshear deformation process can be observed on SEM observations of the specimens surface (Figure 5). From the infrared images it can be observed that the micro-shear deformation process develops on the specimen surface with some heterogeneities that are evidences of an heterogeneous strain distribution along the specimen axis. The scale of the heterogeneities is far above the scale of the inter-space shear band distribution. The final failure occurs in a zone where the thermal evolution is marked by a blow-up like behaviour that overcome the other deformation localisation processes developing along the specimen gage length.

Figure 6 illustrates a 3D tomography image of a tested specimen. The analysed area was chosen according to the infrared image during the tensile test. It is observed that the heat localisation on the IR

image correspond to damage development in the near surface of the specimen. However the damage area is very localized while the microshear process is much largely developed on the specimen surface.

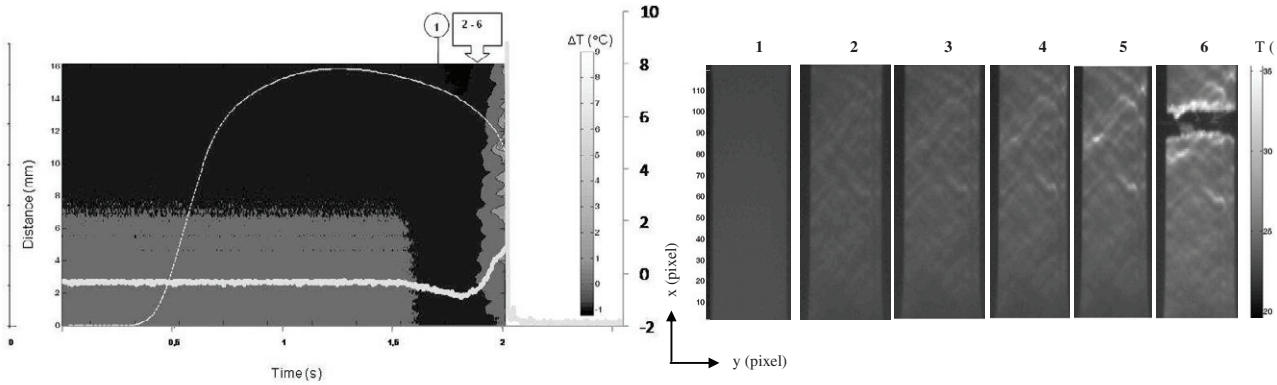

(a) (b)

Fig.3. (a) stress-time evolution (dashed line), mean temperature (solid line) and time evolution of the temperature along the specimen gage length (central line); (b) thermal images at the specimen surface (1pixel represents 0,5mm) for PA66GF20 at a strain rate of 5,5 10^{-2} s^{-1}.

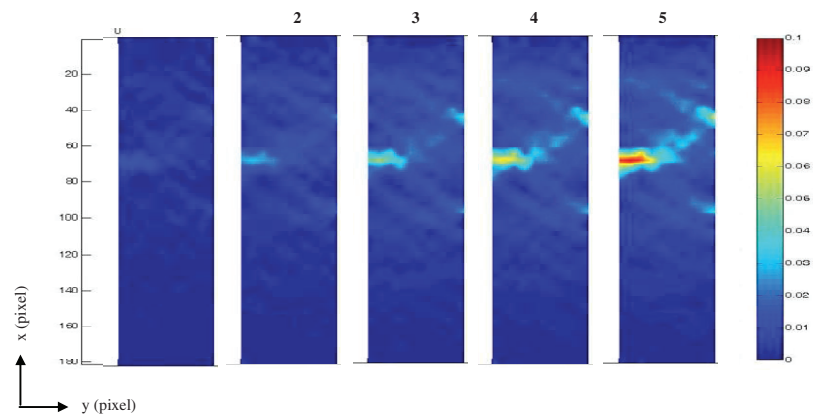

Fig.4. the strain field ε_{11} using 32 pixels elements for PA66GF20 tested at a strain rate of 5,5 10^{-2} s^{-1}.

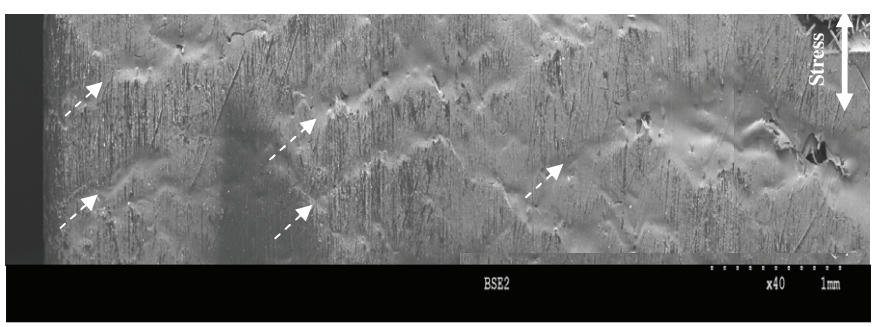

Fig.5. band of microshears in the matrix region.

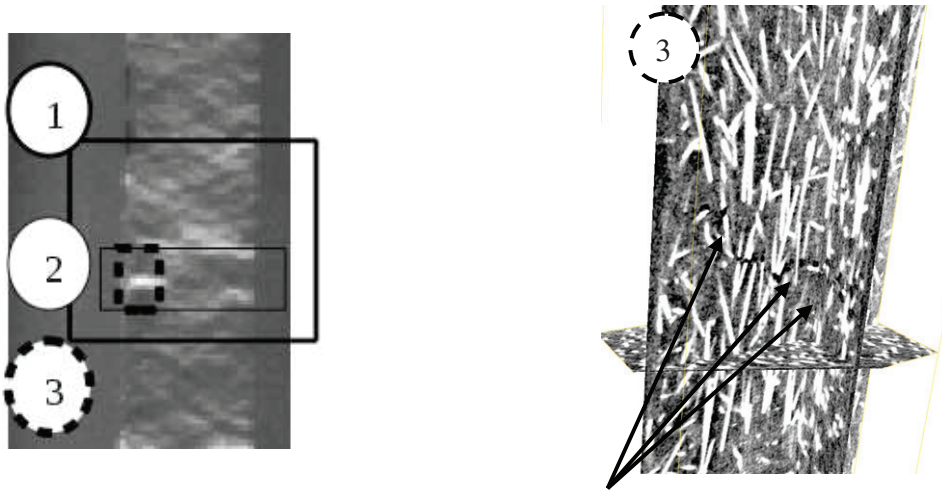

(a) (b)

Fig.6. IR thermal image and corresponding 3D tomography imaging in area 3 indicating that the heat dissipation area observed on figure (a) corresponds to a damage zone development in the near surface of the specimen.

4. Conclusions

The tensile behaviour of glass fibre reinforced and unreinforced polyamide 66 was investigated with infrared thermography, DIC and x-ray computed microtomography methods. Infrared thermography was found to be an efficient tool for investigating the deformation and damage scenario under monotonic tensile loading. Deformation processes once the ultimate tensile stress si reached are mostly governed by microshear deformation that are widelly spread out along the specimen gage length. However IR analyses shows that the microshear deformation process is not uniform along the specimen axis and shows some spatial heterogeneity. The failure processes occurs in zones exhibiting a blow-up type behavior of the thermal signal and are associated to the development of damage which seems to appear only in the very last stage just before failure. Micro-shear deformation processes seem to dominate and control the failure behavior of the material.

References

[1] M.P. Luong, Infrared thermovision of damage processes in concrete and rock, Engineering Fracture Mechanics 35 (1/2/3) (1990) 291-301.

[2] Meola C, Carlomagno GM. Recent advances in the use of infrared thermography. Meas Sci Technol 15 (2004) 27-58.

[3] Mathieu A, Matteï S, Deschamps A, Martin B, Grevey D. Temperature control in laser brasing of a steel/aluminium assembly using thermographic measurements, NDT & E Int 39 (2006) 272-6.

[4] Chrysochoos A. Infrared thermography, a potential tool for analysing the material behaviour. Mecan Indus (2002) 3, 3-14.

[5] Baruchel J, Buffière JY, Maire E, Merle P, Peix G. X-ray tomography in material science. Paris: Herme`s Sciences Publication; 2000. p. 204.

[6] Babout L, Maire E, Buffière JY, Fougères R. Characterization by X-ray computed tomography of decohesion, porosity growth and coalescence in model metal matrix composites. Acta Mater 2001;49:2055–63.

[7] Stanley JH, Computed tomography: the physical and mathematical basis of a powerful new industrial inspection technique. ASTM Standard News (1988) 44–9.